

1-1-1995

## SABER Instrument Design Update

Roy Esplin  
*Utah State University*

Lorin Zollinger  
*Utah State University*

Clair Batty  
*Utah State University*

Steve Folkman  
*Utah State University*

Mehrdad Roosta  
*Utah State University*

Joe Tansock  
*Utah State University*

*See next page for additional authors*

Follow this and additional works at: [https://digitalcommons.usu.edu/sdl\\_pubs](https://digitalcommons.usu.edu/sdl_pubs)

---

### Recommended Citation

Esplin, Roy; Zollinger, Lorin; Batty, Clair; Folkman, Steve; Roosta, Mehrdad; Tansock, Joe; Jensen, Mark; and Stauder, John, "SABER Instrument Design Update" (1995). *Space Dynamics Lab Publications*. Paper 40.

[https://digitalcommons.usu.edu/sdl\\_pubs/40](https://digitalcommons.usu.edu/sdl_pubs/40)

This Article is brought to you for free and open access by the Space Dynamics Lab at DigitalCommons@USU. It has been accepted for inclusion in Space Dynamics Lab Publications by an authorized administrator of DigitalCommons@USU. For more information, please contact [digitalcommons@usu.edu](mailto:digitalcommons@usu.edu).

---

## Authors

Roy Esplin, Lorin Zollinger, Clair Batty, Steve Folkman, Mehrdad Roosta, Joe Tansock, Mark Jensen, and John Stauder

### **SABER instrument design update**

Roy Esplin, Lorin Zollinger, Clair Batty, Steve Folkman, Mehrdad Roosta, Joe Tansock, Mark Jensen, John Stauder  
Space Dynamics Laboratory / Utah State University  
1695 North Research Park Way  
Logan, UT 84341

Jim Miller, Michael Vanek, Don Robinson  
NASA Langley Research Center  
Hampton, VA 23681-0001

### **ABSTRACT**

This paper describes the design of a 10-channel infrared (1.27 to 16.9  $\mu\text{m}$ ) radiometer instrument known as SABER (sounding of the atmosphere using broadband emission radiometry) that will measure earth-limb emissions from the TIMED (thermosphere-ionosphere-mesosphere energetics and dynamics) satellite. The instrument telescope, designed to reject stray light from the earth and the atmosphere, is an on-axis Cassegrain design with a clam shell reimager and a one-axis scan mirror. The telescope is cooled below 210 K by a dedicated radiator. The focal plane assembly (consisting of a filter array, a detector array, a Lyot stop and a window) is cooled to 75 K by a miniature cryogenic refrigerator. The conductive heat load on the refrigerator is minimized by a Kevlar support system that thermally isolates the focal plane assembly from the telescope. Kevlar is also used to thermally isolate the telescope from the spacecraft. Instrument responsivity drifts due to changes in telescope and focal plane temperatures as well as other causes are neutralized by an in-flight calibration system. The detector array consists of discrete HgCdTe, InSb and InGaAs detectors. Two InGaAs detectors are a new long wavelength type, made by EG&G, that have a long wavelength cutoff of 2.33  $\mu\text{m}$  at 77 K.

**Keywords:** SABER, TIMED, BRDF, radiometer, earth-limb, kevlar, refrigerator, stray-light

### **1. INTRODUCTION**

SABER (sounding of the atmosphere using broadband emission radiometry) is an earth-limb-scanning radiometer that has been selected as one of the four payload instruments on TIMED (thermosphere-ionosphere-mesosphere energetics and dynamics) satellite to be launched in October 1998. The TIMED orbit altitude is 600 km and the orbit inclination is 74.4 degrees. SABER will look 90 degrees to the ram. The mission life is 2 years.

The SABER systems requirement review (SRR) and the conceptual design review (CoDR) were held in April 1995, and the preliminary design review is scheduled for April 1996. Significant modifications to the SABER design described in the literature<sup>3</sup> have been made in the last year. Many of these modifications resulted because the previous optical design required filters that were impractically thick to correct for chromatic focal shifts across the very wide spectral band covered by SABER. A new optical design that solved this problem and resulted in a much more rugged instrument was developed and is described in this paper. The stray light performance of this new design is excellent. This paper is intended to provide a comprehensive overview of the new SABER design.

### **2. SYSTEM DESIGN**

A functional diagram of the SABER instrument is shown in Figure 1. A high off-axis rejection telescope collects wanted light and discriminates against unwanted light. The scan mirror scans the instrument field of view vertically across the earth limb. In orbit the telescope is oriented so the nadir-zenith line is vertical in Figure 1 and local depression angles are measured relative to the horizontal. The baffle opening allows the center of SABER's 1.4 degree wide field of view to be scanned across depression angles from 11.148 to 26.168 degrees. This allows SABER to look from cold space down to the hard earth. The depression angle of the input baffle axis, the angle of the input rays in Figure 1, is 18.658 degrees. The scan mirror operates in two data taking modes: an acquisition mode that locates the region of the earth limb to be measured by over scanning, and an adaptive mode that maximizes data taking efficiency by locking onto the required measurement region and reducing the scan amplitude. When in the adaptive mode, the scan mirror turns so SABER views the full aperture blackbody and cold space every other scan cycle. This approach provides in-flight calibration (IFC) of the long wavelength channels. Less frequently the scan mirror rotates so SABER views the tungsten lamps, which serve as calibration sources for the short wavelengths. Mirrors M1 and M2, which are arranged in a Cassegrain configuration, focus input light onto an intermediate focal plane where a chopper modulates light from within the field of view and blocks light from outside the field of view.

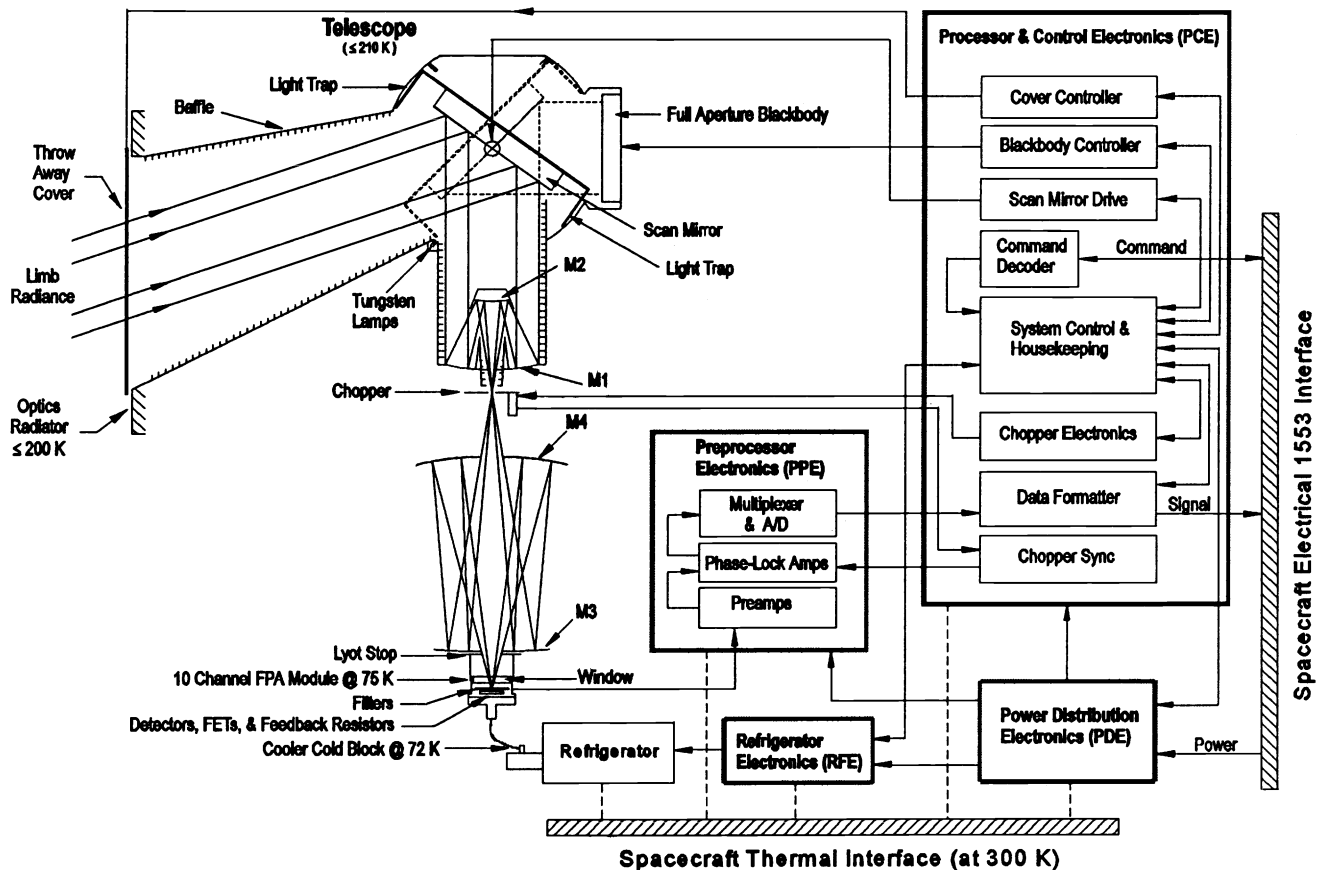


Figure 1. SABER instrument functional diagram

This modulated light is refocused on an array of ten discrete detectors by means of mirrors M3 and M4, which are arranged in a clam-shell configuration. An array of ten optical bandpass filters limit the spectral bandwidth of light reaching each detector. The detectors and filters are protected from contamination by a KBr window. Stray light from outside the field of view is blocked by baffles, the chopper and a Lyot stop. The electrical signal from the ten detectors is amplified and synchronously demodulated by means of ten phase-lock amplifiers that are synchronized with the chopper. The demodulated outputs from the phase-lock amplifiers are multiplexed through one analog-to-digital converter. The digitized data are then formatted together with housekeeping data and picked up by the spacecraft by means of a 1553 electrical interface. The focal plane assembly, which consists of the detector array, the filter array, window and Lyot stop, is cooled to 75 K by a miniature TRW refrigerator to reduce photon noise and thermally generated noise in the detectors. The telescope is cooled below 210 K by means of a dedicated radiator to reduce photon noise, reduce the heat load on the refrigerator, and to minimize the temperature of the full aperture blackbody. The electronics boxes and the refrigerator are attached to the instrument mounting plate that is cooled to between 250 K and 300 K by the spacecraft. A throw-away cover protects the optics from contamination during ground and launch operations. SABER has electronic controllers for the refrigerator, scan mirror, chopper and cover release. The command decoder and system controller are state machines implemented in programmable logic. This approach offers radiation hardness and minimizes costly software efforts. Flexibility is achieved by using state machines to call other state machine modules. The system controller provides seven instrument operational modes: off, warm-up, calibrate, data collection, standby, stabilization, diagnostic/reprogram.

The in-flight calibration (IFC) system provides correction for changes in instrument responsivity and offset caused by changing conditions such as changes in the temperature of the telescope, focal plane, and electronics as well as optical transmission changes. The cold space measurement provides a measurement of the instrument offset. The instrument radiance responsivity is given by

$$R = \frac{V_{IFC} - V_S}{L_{IFC}} \quad (1)$$

and the earth-limb radiance is given by

$$L_L = \frac{V_L - V_S}{R} = \frac{(V_L - V_S)}{(V_{IFC} - V_S)} L_{IFC} \quad (2)$$

where  $R$  is the radiance responsivity,  $L_L$  is the limb radiance,  $L_{IFC}$  is the in-flight calibrator radiance and  $V_L$ ,  $V_S$ , and  $V_{IFC}$  are the corrected signal voltages (corrected for nonlinearity, etc., from ground calibration data) when SABER is viewing the earth limb, cold space, and the IFC, respectively.

The fractional radiance error due to errors in each of the four variables in Equation 2 can be found by differentiating with respect to the variable and dividing by the limb radiance. If the errors are assumed to be uncorrelated, the total error is the root sum square of the individual errors and the total fractional radiometric error is given by

$$\frac{\Delta L_L}{L_L} = \sqrt{\left[ \frac{\Delta V_L}{V_L - V_S} \right]^2 + \left[ \frac{\Delta V_{IFC}}{V_{IFC} - V_S} \right]^2 + \left[ \frac{(V_S - V_{IFC}) \Delta V_S}{V_{IFC} - V_S (V_L - V_S)} \right]^2 + \left[ \frac{\Delta L_{IFC}}{L_{IFC}} \right]^2} \quad (3)$$

where  $\Delta V_L$ ,  $\Delta V_{IFC}$ , and  $\Delta V_S$  are the errors in the corrected measurement voltages of the earth limb, the IFC source, and cold space, respectively, and  $\Delta L_{IFC}$  is the radiance error of the IFC. Ground calibration errors are included in  $\Delta V_L$ ,  $\Delta V_{IFC}$ , and  $\Delta V_S$  as correction residuals and in  $\Delta L_{IFC}$  as errors in the radiance estimate of the ground blackbody source and in the transfer to the IFC source. For signal-to-noise ratios greater than 100, the absolute radiance calibration requirement for SABER is 5% with a goal of 3% and the long term radiometric precision requirement is 2% with a goal of 1%.

The atmospheric species measured, spectral passbands, filter materials, detector materials and Noise Equivalent Radiance (NER) values for each channel are tabulated in Table 1. Channels 2 and 3 have identical spectral passbands; their different locations provide a means for correcting spacecraft pointing variations.

**Table 1.** Summary of channel parameters

Channel Number	Channel Name* (Based on Atmospheric Species Measured)	Spectral Passband Half Power Points ( $\mu\text{m}$ )	Filter Substrate Material	Detector Material and Operating Mode**	Noise Equivalent Radiance, NER ( $\text{Wcm}^{-2}\text{sr}^{-1}$ )
1	CO <sub>2</sub> - N	14.888 - 15.520	InSb	MCT PC	1.70E-8
2	CO <sub>2</sub> - W	13.347 - 16.941	InSb	MCT PC	2.80E-8
3	CO <sub>2</sub> - W	13.347 - 16.941	InSb	MCT PC	2.80E-8
4	O <sub>3</sub>	9.057 - 9.729	Ge	MCT PC	1.10E-8
5	H <sub>2</sub> O	6.510 - 7.120	Ge	MCT PC	3.70E-9
6	NO	5.257 - 5.566	Sapphire	InSb PV	2.50E-9
7	CO <sub>2</sub> - B	4.197 - 4.350	Sapphire	InSb PV	1.30E-9
8	OH - A	1.952 - 2.189	Sapphire	LW InGaAs PV	4.70E-10
9	OH - B	1.562 - 1.698	Sapphire	LW InGaAs PV	4.70E-10
10	O <sub>2</sub>	1.262 - 1.285	Sapphire	InGaAs PV	4.70E-10

\* Channel name abbreviations: N = narrow, W = wide, A = first, B = second

\*\* Detector mode and material abbreviations: PV = photovoltaic mode, PC = Photoconductive mode, MCT = mercury cadmium telluride, LW = long wavelength

The long wavelength InGaAs detectors used for channels 8 and 9 are a new type developed recently by EG&G. At 77 K these detectors have been demonstrated to have a long wavelength cut off of  $2.33\text{ }\mu\text{m}$ , a quantum efficiency of 50, a  $R_0A$  product of  $2\text{E}7$  to  $2\text{E}8$  and a capacitance of  $0.3\text{E}-8$  to  $0.7\text{E}-8\text{ f/cm}^2$ .

The SABER instrument weighs 58.5 kg, requires an envelope  $0.9\text{ m} \times 0.6\text{ m} \times 0.5\text{ m}$ , requires 59.5 watts of power and has an output data rate of 4000 bits per second. The nominal footprint of the instantaneous field of view (IFOV) of each detector at the earth limb is 2 km vertical by 28 km horizontal. The sample rate is 5 samples per vertical IFOV.

The SABER instrument is a single integrated unit as shown in the two three-dimensional views given in Figure 2. The instrument mounting plate, optics radiator, telescope, Kevlar telescope support hubs, refrigerator, focal plane assembly, and electronics boxes are identified in these figures. The SABER instrument is bolted to the spacecraft at the mounting plate which also serves as a thermal connection to the spacecraft for cooling the electronic boxes and refrigerator mounted on it. The Kevlar fibers in the telescope support

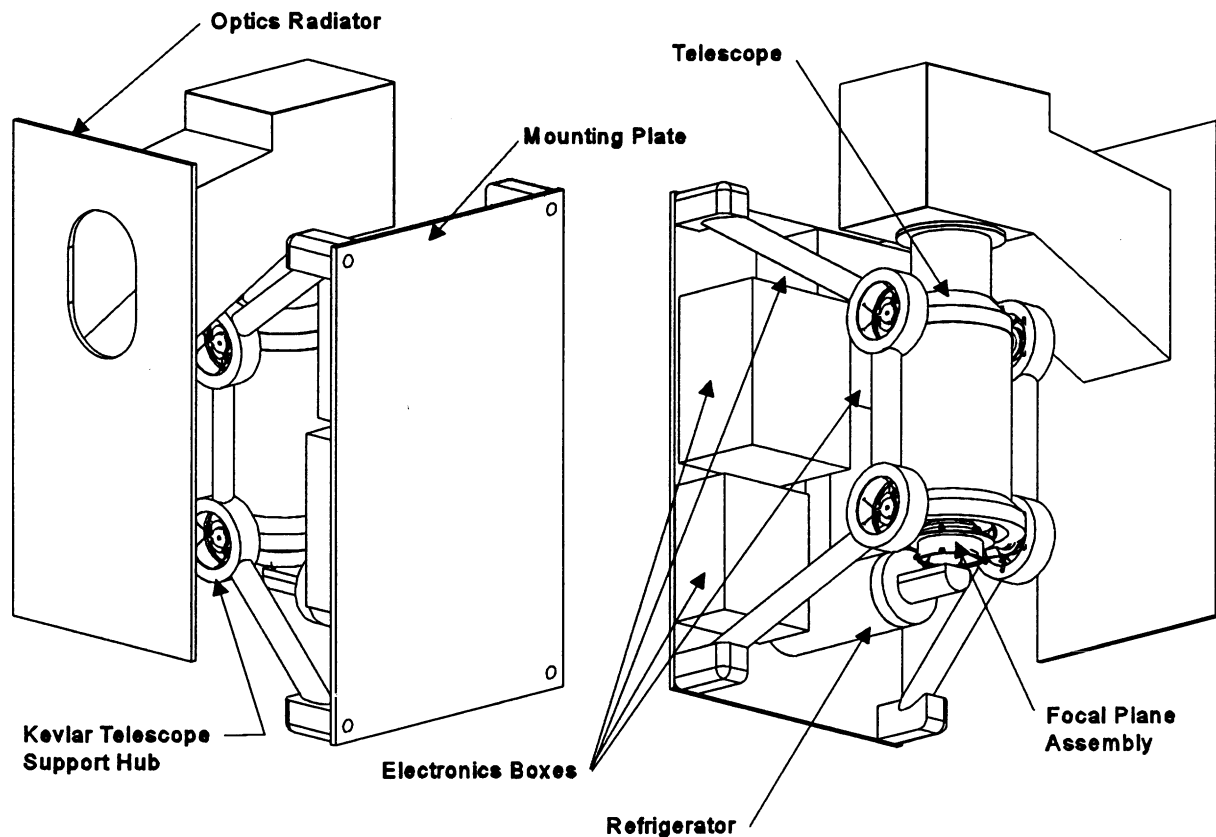


**Figure 2.** SABER instrument

hubs thermally isolate the telescope from the spacecraft and provide a very stiff support system. The telescope housing, baffle, and radiator are fabricated from aluminum. The structural design is driven by design load and minimum frequency requirements. The TIMED spacecraft minimum frequency requirements are 70 Hz in the thrust axis and 50 Hz in the lateral axis. A preliminary finite element model of the instrument was assembled and resonant modes examined. This effort demonstrated that the support system can maintain the resonant frequencies above 70 Hz. The most flexible component in the system is the radiator panel. To improve its rigidity ribs will be machined into its back face and additional connections will be made to the telescope. The focal plane assembly is thermally isolated from the telescope by a Kevlar support system. A detailed three-dimensional drawing of the focal plane assembly and its Kevlar support system is shown in Figure 3. These Kevlar strands provided excellent thermal isolation and provide an extremely stiff support system. The resonant frequency of a prototype FPA support system was measured and found to exceed 600 Hz. The detector array, filter array, window, Lyot stop and mounting surface are identified in the cross-sectional view of the focal plane assembly and its Kevlar support system shown in Figure 4. The FPA is aligned to the telescope by making adjustments between this mounting surface and the telescope.

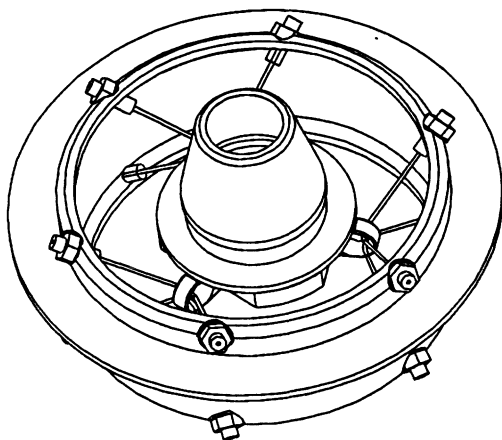


**Figure 3.** FPA and support system three-dimensional view

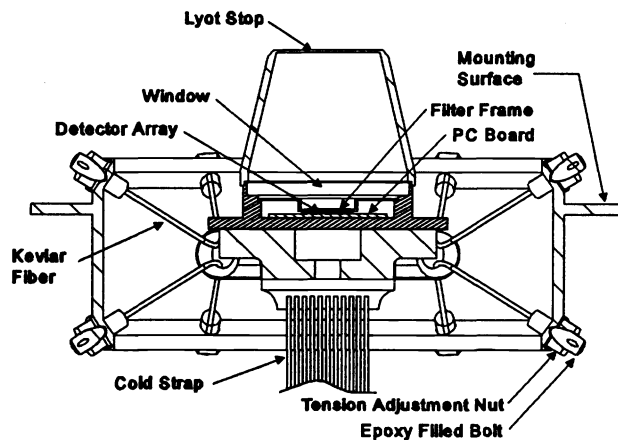


**Figure 4.** FPA and support system sectional view

### 3. SABER THERMAL MANAGEMENT

#### 3.1 Thermal Overview

The SABER thermal management plan is illustrated schematically in Figure 1. The focal plane assembly (FPA) is cooled to 75 K using a TRW miniature pulse tube refrigerator. The telescope, thermally isolated from the spacecraft and cooled by an independent radiator, will operate between 195 K and 210 K. The refrigerator and all electronics boxes are mounted on an interface plate attached directly to the spacecraft and is expected to operate between 250 K and 300 K.

#### 3.2 Refrigerator

The TRW miniature pulse tube refrigerator was selected for its small size, low mass, low input power requirements, low vibration, long life and high reliability. This refrigerator, based on the Oxford non-wear bearing technology, is the result of seven years of development for the Brilliant Pebbles program. Some of the basic refrigerator parameters\* are summarized in Table 2.

**Table 2.** Refrigerator parameters

Parameter	Value
Refrigerator Mass Electronics Mass	2 kg 3 kg
Refrigerator Footprint Electronics Footprint	50 in. <sup>2</sup> 55 in. <sup>2</sup>
Refrigerator Rated Power Input Electronics Rated Power Input	20 W 7W
Cooling Capacity at 72 K with 20 W input and 300 K reject temperature	250 mW
Vibration Imposed Force	< 0.02 lbf rms
Predicted Life/ Reliability ( includes electronics)	> 5 years/0.96 > 10 years/0.919

\* Contact Dr. William W. Burt of TRW at (310) 812- 0411 for additional information regarding this refrigerator.

### 3.3 Refrigerator Heat Loads

The heat loads to the refrigerator must be kept below its 250 mW capacity to ensure the focal plane temperature does not exceed 75 K. These heat loads are summarized in Table 3.

The Kevlar support system makes this SABER instrument possible. With conventional supports and geometric constraints on support length in this application, parasitic conduction would cause the refrigerator heat loads to exceed the capacity of the miniature refrigerator. Larger refrigerators with greater cooling capacity would impose unacceptable power requirements on the spacecraft.

### 3.4 Telescope Radiator

The telescope radiator is required for two reasons. The signal-to-noise ratio becomes unacceptable as the optics temperature exceeds about 220 K. Also, the radiation heat load to the refrigerator via the cold stop aperture quickly becomes excessive at temperatures above this level. The telescope radiator is sized (area = .28 m<sup>2</sup>) to keep telescope temperatures below 210 K even at end of mission life with normal surface degradation.

### 3.5 Heat Loads to Telescope Radiator

The telescope radiator heat load is kept as low as possible to minimize radiator area. Only those heat sources, as listed in Table 4, that are not separable from the telescope are cooled via this radiator. All other heat sources are cooled at higher temperatures via the spacecraft.

### 3.6 Spacecraft Mounting Plate and Radiator

All major heat sources not an integral part of the telescope are cooled through the spacecraft mounting plate expected to operate between 250 K and 300 K. This mounting plate, having an area of 0.4 m<sup>2</sup>, will conduct 55.6 watts (see Table 5) to the spacecraft and then radiate the heat to space.

## 4. OPTICAL SYSTEM

The optical system was designed to satisfy the following requirements: the optical system must have 1) a 2 km wide detector footprint at the earth limb, 2) must fit in TIMED spacecraft and survive the shake requirements, 3) a spot size smaller than the detector width, high transmission and good filtering for channels scattered across the wavelength band from 1.26 to 16.9  $\mu\text{m}$ , 4) a field of view large enough to accommodate 10 detectors, 5) a cryogenically rugged filter assembly, 6) a f-number  $\leq 2$ , 7) high stray-light rejection, 8) a cold Lyot stop, and 9) a chopper. To obtain the required wide spectral coverage with high transmission

**Table 3.** Refrigerator heat loads

Heat Load Source	Power (mW)
Radiation via cold stop aperture	50
Radiation via MLI blankets	70
Conduction via wires	35
Detector power	50
Conduction via Kevlar tension supports	2
Margin	43
Total	250

**Table 4.** Telescope radiator heat loads

Heat Load Source	Power (watts)
Scan Motor, encoder	2.50
Radiation from spacecraft via MLI blankets	1.00
Conduction via Kevlar supports	0.10
Calibration Blackbody	1.00
Chopper	0.40
Margin	1.00
Total	6.00

**Table 5.** SABER component power dissipation

SABER Component	Power (watts)
Refrigerator	20.00
Preprocessor Electronics (PPE)	8.80
Power Distribution Electronics (PDE)	6.50
Processor & Control Electronics (PCE)	13.30
Refrigerator Electronics (RFE)	7.00
Total	55.60



optical systems and lens proved impractical. In addition, the high stray-light requirement prohibited optical systems with a lens illuminated by off-axis light. Off-axis reflective optical systems offered the required high stray-light performance, but our best off-axis design had a f-number of 2.3 and it had no room for a chopper. A system with an off-axis front end and a Schwarzschild reimager proved to be too large even when a field mirror was added. On-axis designs offer smaller f-numbers, smaller size, greater ruggedness than off-axis systems, but they are harder to baffle and analyze. Therefore, a detailed stray-light study was conducted using APART<sup>4</sup> to ascertain if the stray-light performance required for SABER could be achieved with an on-axis design. The prescription of the on-axis optical system used in this stray-light study is tabulated in Table 2.

**Table 6.** Optical prescription

Srf. No.	Radius of Curvature (mm)	Thickness (mm)	Glass	Special Data	Notes
1	--	-634.908	--	--	Entrance Pupil
2	--	393.506	--	--	
3	--	--	Reflection	Tilt Angle = 35.671 deg. (nominal)	Scan Mirror
4	--	-82.500	--	Tilt Angle = 35.675 deg. (nominal)	
5	--	-158.902	--	--	
6	225.000	75.000	Reflection	Conic Constant = -1.15149 Aperture Stop Radius = 50.000 mm	Primary Mirror and Aperture Stop
7	120.000	-75.000	Reflection	Conic Constant = -6.62063	Secondary Mirror
8	--	-25.000	--	--	Hole in Primary
9	--	-70.000	--	--	Chopper
10	--	-210.000	--	--	Input Hole
11	1050.000	210.000	Reflection	Conic Constant = -60.08293	Tertiary Mirror
12	-384.407	-210.000	Reflection	Conic Constant = 0.39100	Quaternary Mirror
13	--	-1.130	--	--	Output Hole
14	--	-29.050	--	--	Exit Pupil
15	--	-3.000	KBr	--	Window
16	--	-9.500	--	--	
17	--	-0.500	InSb, Ge or Sapphire	Channels. 1,2,3: InSb Channels. 4,5: Ge Channels 6-10: Sapphire	Filter
18	--	-0.400 or -0.254	--	Channels 1-5: -0.400 Channels 6-10: -0.254	
19	--	--	--	--	Detector

A schematic drawing of this optical system showing its main features and marginal rays is shown in Figure 5. This design has two large stray-light advantages: an intermediate field stop (the chopper) and a Lyot stop. The intermediate field stop prevents off-axis rays from entering the back end of the optical system. The Lyot stop blocks diffraction from the aperture stop and prevents the detectors from seeing anything outside the outer diameters of the optical elements. The central obscuration is defined by the tips of the secondary baffle cone (see Figure 5). The scan mirror, secondary mirror and primary mirror are super polished. The entire secondary mirror front surface is super polished, even though the entire area is not used for specular reflection because it minimizes stray-light reflections. Similarly the outside edge of the primary mirror inner conical baffle (see Figure 5) is moved in radially significantly beyond the spectral rays because the light scattered from the low BRDF mirror surface is much less than that scattered from a painted surface. The APART stray-light modeling performed for this study was independently reviewed by Breault Research Organization, Inc. who suggested the outside edge of the inner conical baffle be moved as described above. The results of this stray-light study show that for this optical design the scattered light from the earth and the atmosphere is negligible. This stray-light study is described in greater depth in a companion paper<sup>5</sup>. This optical design satisfies all nine optical system requirements listed above.

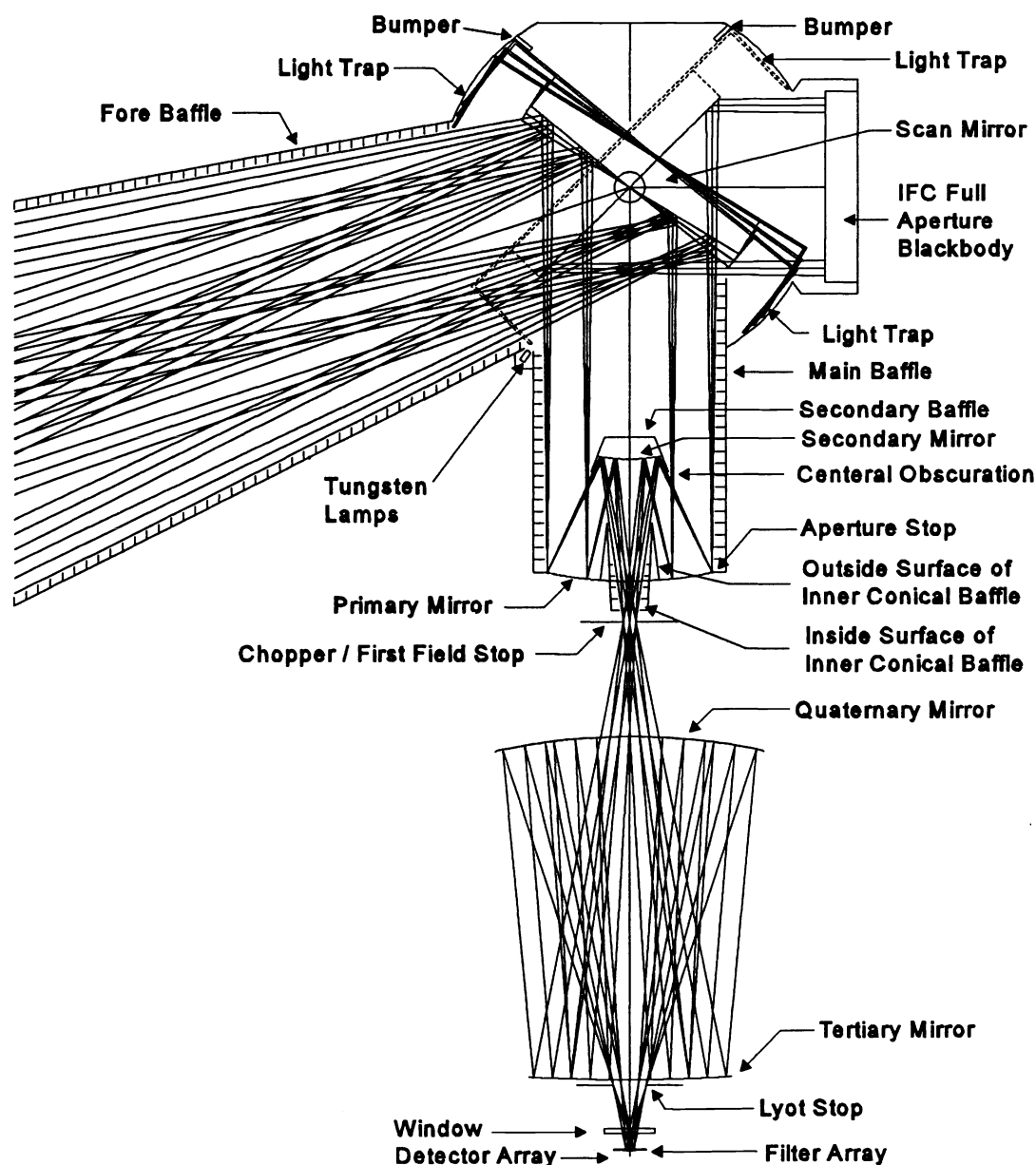


**Figure 5.** SABER optical system

The required field of view of the optical system is driven by the mechanical technology used to produce the filter assembly, the f-number of the optical cone, the filter thickness, and the distance between the filter and detector. In order to minimize FPA size the filters were made as thin as possible (0.5 mm), placed as close as possible (0.254 mm) to the detectors, and supported with minimum web thickness (0.127 mm) between filters. Optical Coating Laboratory, Inc. (OCLI) supplied the dimensions required for adhesive and chips on the filter edges. The dimensions of the resulting filter assembly are shown in Figure 6. The top plate which covers the filter edges is not shown in this drawing. OCLI fabricated and successfully cryogenically tested a breadboard using indium antimonide, germanium and sapphire substrates, sized similar to the required filters, and mounted in a molybdenum frame. A finite element model was made to verify the structural rigidity of the filter assembly. This model passed the 16 g load requirements with margins of safety greater than 16 with a safety factor of 2.

The detector assembly dimensions determined the filter spacings as shown in Figure 7. Given the 200 mm focal length of the telescope the detector array field of view is 1.4 by 1.4 degrees. As shown in this figure, the detector dimensions are 0.140 mm by 2.000 mm. In order to maximize sensitivity the detectors serve as the field stop since this minimizes detector size and most detector noise processes increase with detector area. Figure 7 also shows the relative location of the ten channels at the focal plane. This drawing also represents the relative location of the ten channel footprints at the earth limb viewed looking out of the SABER aperture with down being in the direction of the earth (the earth is down in Figure 5).

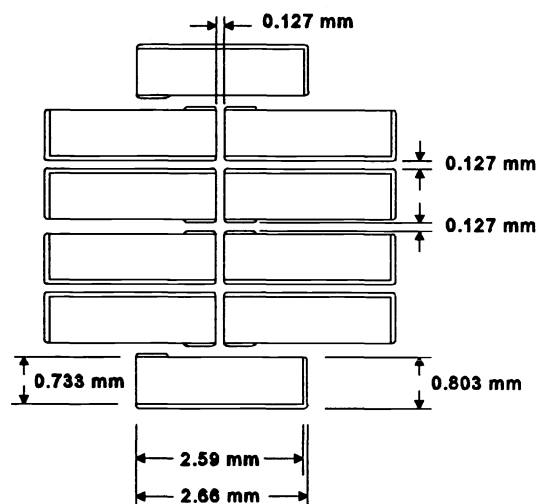


**Figure 6. Filter array layout**

Schematic diagram of the sample layout for the experiment. The diagram shows a central grid of nine sample positions, numbered #1 to #9. Each position contains a sample with a specific chemical composition and a wavelength value. The samples are arranged in a 3x3 grid. The top row contains #6 NO (5.40  $\mu\text{m}$ ), #7 CO<sub>2</sub> (4.3) (4.27  $\mu\text{m}$ ), and #8 OH (A) (2.06  $\mu\text{m}$ ). The middle row contains #9 OH (B) (1.62  $\mu\text{m}$ ), #10 O<sub>2</sub> (1.27  $\mu\text{m}$ ), and #3 CO<sub>2</sub> W (14.9  $\mu\text{m}$ ). The bottom row contains #4 O<sub>2</sub> (9.39  $\mu\text{m}$ ), #2 CO<sub>2</sub> W (14.9  $\mu\text{m}$ ), and #1 CO<sub>2</sub> N (15.2  $\mu\text{m}$ ). A fifth sample, #5 H<sub>2</sub>O (6.80  $\mu\text{m}$ ), is located below the bottom row, centered between the first and second columns. Dimensions are indicated: a vertical dimension of 1.4 m on the left, a vertical dimension of 4.882 m on the right, and a horizontal dimension of 2.717 m at the bottom. Spacing dimensions are given: 0.140 mm between the bottom row and the #5 sample, 0.961 mm between the top row and the #6 sample, 1.000 mm between the middle and bottom rows, and 0.960 mm between the #3 and #4 samples. A horizontal dimension of 2.000 mm is shown for the #5 sample.

diffraction limited for channels 1 through 5. For channels 6 through 10 the spot is smaller than it is for the long wavelength channels, but it is dominated by geometrical aberrations rather than diffraction. However, the spot width for these channels is less than one-quarter the 0.140 mm detector width. The detectors are on two different levels to compensate for chromatic aberrations in the window and filters. The long wavelength detectors, channels 1 through 5, are located 0.146 mm farther behind the filter array than the short wavelength channels 6 through 10. As can be seen from Figure 7, channels 1 through 5 are located in one contiguous group and 6 through 10 in another contiguous group. This approach makes it easier to fabricate the required two-level focal plane, and fortunately the detectors that require the lowest temperatures are mounted on the shortest standoffs.

**Figure 7. Detector array layout**

**Table 7. Geometrical and diffraction limited spot sizes**

<b>Channel Number</b>	<b>Center Wavelength (μm)</b>	<b>Detector Filter Clearance (mm)</b>	<b>Geometrical Spot Size RMS Radius (mm)</b>	<b>Diffraction Limited Spot Size Radius (mm)</b>
1	15.38	0.400	0.0116	0.0372
2	14.93	0.400	0.0083	0.0362
3	14.93	0.400	0.0083	0.0362
4	9.4	0.400	0.0082	0.0228
5	6.8	0.400	0.0122	0.0164
6	5.4	0.254	0.0164	0.0131
7	4.3	0.254	0.0110	0.0104
8	2.06	0.254	0.0098	0.005
9	1.63	0.254	0.0083	0.00395
10	1.27	0.254	0.0085	0.0031

## **5. CONCLUSIONS**

The SABER instrument has been selected for flight on the TIMED spacecraft in 1998. Instrument design has advanced past the conceptual design review; the preliminary design review is scheduled for April 1996. The wide spectral coverage required in SABER made it necessary to change the optical system to an all reflective design. Stray-light studies have shown that the SABER stray-light rejection requirements can be met with a carefully baffled on-axis system that has an intermediate field stop and a Lyot stop.

The SABER instrument will advance both scientific knowledge and space engineering technology. Science knowledge of the mesosphere and thermosphere will be advanced by the long-term global monitoring of the mesosphere and thermosphere that SABER will provide. Space engineering technology will be advanced by the opportunity SABER offers to demonstrate several new technologies in space: TRW's miniature cryogenic refrigerator, Kevlar thermal-isolation support systems, a miniature cryogenic assembly of discrete optical filters made with several infrared substrate materials, and InGaAs detectors with extended long wavelength response to 2.3 μm at 77 Kelvins.

## **6. ACKNOWLEDGEMENTS**

The work reported in this paper has been supported by NASA contract NAS1-20080. Follow-on SABER work has begun under NASA contract NAS1-20476. TRW has provided information on their miniature cryogenic pulse tube refrigerator and supported breadboard testing of the Kevlar support system and thermal straps, EG&G has provided detector modeling and information including information on its recently developed long wavelength cutoff InGaAs detectors, Optical Coating Laboratory, Inc. provided a base line miniature filter assembly design and performed cryogenic testing on a filter breadboard assembly, and Breault Research Organization, Inc. reviewed APART stray-light analysis and made design recommendations. The mechanical design drawings were done by Dave McLain and Peter Brunson of SDL.

## 7. REFERENCES

1. R. Esplin *et. al.*, "SABER instrument overview," *SPIE Proceeding*, Vol. 2268, pp. 207- 217, 1994.
2. R. Esplin *et. al.*, "A Satellite-based Multichannel Infrared Radiometer to Sound the Atmosphere (SABER)," OSA 1995 Technical Digest Series Vol 2, Optical Remote Sensing of the Atmosphere pp 130-132, 1995.
3. J.C. Batty *et. al.*, "Cooling SABER: interface performance and design issues," *SPIE Proceedings*, Vol 2227, pp 199-210, 1995.
4. "APART Stray Light Analysis Software Package, Version 9.3," Breault Research Organization 6400 East Grant Road, Suite 350, Tucson Arizona, 85715.
5. J. Stauder *et. al.*, "Stray light analysis of the SABER telescope," *SPIE Proceeding*, Vol. 2553, 1995.